The Presolvated Electron in Water: Can It Be Scavenged at Long Range?†

Qing-Bin Lu,‡ J. Spencer Baskin, and Ahmed H. Zewail*

Laboratory for Molecular Sciences, Arthur Amos Noyes Laboratory of Chemical Physics, California Institute of Technology, Pasadena, California 91125

Received: January 30, 2004

Femtosecond transient absorption measurements were carried out to investigate the scavenging effect, at low concentration, of the radiosensitizing molecule 5-bromo-2′-deoxyuridine (BrdU) on presolvation states of the hydrated electron. Hydrated electrons were generated by two photon absorption of bulk water at 267 nm, and transient absorption at 1200 nm was monitored. Results from experiments performed with the sample in a 5-mm cell showed a dramatic BrdU concentration dependence strongly suggestive of dynamic scavenging of the presolvated electron observable at concentrations as low as 0.2 mM, but no scavenging was detected in experiments on a thin sample jet with BrdU concentrations of up to 10 mM. Further analysis reconciled these results, confirming the absence of scavenging and attributing the concentration effect in the cell measurements to a group-velocity-dispersion-induced concentration dependence of the temporal response function. However, low concentrations of BrdU were seen to enhance the generation of hydrated electrons for excitation at both 267 and 310 nm.

I. Introduction

It has been known for decades that free electrons can be trapped in polar solvents such as ammonia and water. These solvated electrons (e_{solv}^-) are a major product in radiation chemistry and play an important role in diffusive electron-transfer reactions and biological radiation effects. A great deal of information is known about the solvated electron and its chemistry.[1] With the birth of ultrafast laser spectroscopy, the solvation dynamics of electrons in liquid water has been studied in some detail over the past decade. (See, for example, refs 2−11.) It is now known that electron solvation occurs through multiple stages, depending on the initiation process. When the electron is produced by two-photon absorption of UV light by pure water, as many as five distinct stages have been proposed[9,10] to account for the complex and varied transient behavior observed at wavelengths from the visible up to 7 μm in the IR.[11] Theoretical treatment of the problem has elucidated the microscopic picture. (See, for example, refs 12 and 13).

The exact physical nature of the short-lived (<1 ps) transient states through which the electron passes before becoming fully solvated, denoted collectively as e_{pre}^- hereafter, is still the subject of investigation; some evidence suggests that among these states is one in which the electron is localized in a weakly bound preexisting trap related to the Urbach tail extending below the water conduction band as a result of electron−phonon interactions.[14−16] Nevertheless, e_{pre}^- is generally believed to be highly reactive and to play a significant role in radiation-induced reactions of molecules in polar media. For example, it has been proposed that e_{pre}^- in ice is responsible for the strong enhancement of the dissociation of chlorofluorocarbons (CFCs) adsorbed on ice surfaces,[17] which is of high relevance to the formation of the ozone hole in earth's atmosphere.[18] However, the reaction of e_{pre}^- is difficult to observe directly because of its ultrashort lifetime, on the femtosecond time scale. So far, e_{pre}^- reactivity with electron scavengers has been derived only indirectly from measurements of yields of the solvated electron (e_{solv}^-) on the picosecond time scale with scavengers at concentrations in excess of 0.1 M.[19−21]

In an effort to see if the effect of scavenging could be directly observed in the time evolution of e_{pre}^-, we have performed femtosecond transient absorption experiments with 5-bromo-2′-deoxyuridine (BrdU) serving as the scavenger. In view of the importance of ultrafast (picosecond and femtosecond) electron-transfer processes in biological systems studied in this laboratory,[22,23] the reduction of such organics by a free electron could be of relevance to processes involving reactions, for example, with bases in DNA. BrdU is a sensitizer used in radiobiology and a probe for structural studies of nucleic acids and their interactions with proteins.[24,25] In these applications, the first and critical step is electron transfer to BrdU to produce the highly reactive uracilyl radical that then dissociates.[26] The large electron-capture cross section manifested by BrdU in such studies led us to choose it for the e_{pre}^- scavenging experiments at low concentration to address the possibility of long-range reaction by, for example, tunneling or the effect of the diffuseness of excited electron states.[21] With the generic scheme of Figure 1 representing the basic elements of the electron generation and solvation process in pure water, the steps relevant to the femtosecond experiments are

$$\text{without BrdU: } H_2O \xrightarrow{2h\nu} H_2O^* \xrightarrow{k_1} e_{pre}^- \xrightarrow{k_2} e_{solv}^- \quad (1)$$

$$\text{with BrdU: } e_{pre}^- + \text{BrdU} \xrightarrow{k_3} \text{BrdU}^{*-} \rightarrow Br^- + dU^\bullet \quad (2)$$

where the bimolecular scavenging rate, k_3, is proportional to the BrdU concentration. In this model, the transient signal of e_{pre}^- rises at rate k_1 and has a decay rate of k_2 (for $k_1 > k_2$) in pure water, increasing to $k_2 + k_3$ as the scavenging channel is opened. Scavenging of e_{solv}^- is also expected but could occur

† Part of the special issue "Gerald Small Festschrift".

* Corresponding author. E-mail: zewail@caltech.edu.

‡ Present address: Department of Physics, University of Waterloo, Waterloo, Ontario, Canada N2L 3G1.

10.1021/jp0400824 CCC: $27.50
Published on Web 04/03/2004

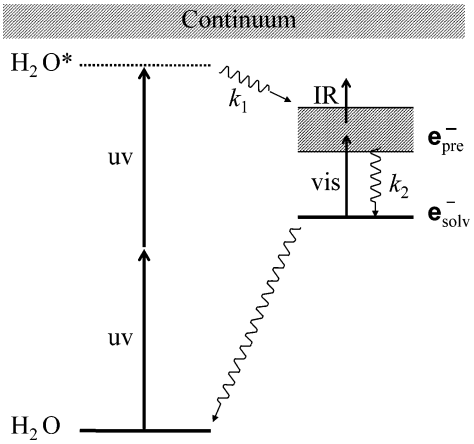

Figure 1. Simplified model for the generation of the hydrated electron by the excitation of water by two UV photons. The absorption of the equilibrated hydrated electron (e_{solv}^-) with a maximum at 720 nm is assigned to a transition from an s-like ground state to three nearly degenerate p states. The latter are among states that have been assigned as presolvation intermediates (e_{pre}^-) for a variety of electron production routes. In these higher excited states, the electron distribution is much more diffuse than in the ground state.[21]

on a much longer time scale (nanoseconds or greater) and is not of interest here.

II. Experimental Results and Discussion

Initially, a standard methodology for femtosecond (fs) transient absorption measurements[22,23] was used on ultrapure water samples (resistivity > 18 MΩ/cm, obtained directly from a Barnstead Nanopure cartridge system) in a 5-mm path length quartz cell. The pump (267 nm, 0.5−4.5 μJ) and tunable probe pulses (<0.01 μJ) were derived from a femtosecond Ti:sapphire laser system by frequency tripling and optical parametric amplification, respectively. The two beams were focused through a single quartz lens, and the cell was positioned where the beams were of similar cross section with diameters of ∼0.6−1.0 mm.

Whereas water is transparent to one-photon absorption at 267 nm, the absorption of two pump photons (9.3 eV) leads with fairly high efficiency to the ejection of an electron[27] and the initiation of the electron solvation sequence. Measured transient absorption spectra for pure water with $\lambda_{probe} = 1200$ and 620 nm are shown in Figure 2. These spectra agree qualitatively with expectations based on the general trends reported in the literature at a variety of probe wavelengths.[2−11] That is, the signal for IR probing (Figure 2a) is dominated by a subpicosecond rise and decay attributed to e_{pre}^-, and the visible probe-wavelength signal (Figure 2b), which rises more slowly to a plateau on the time scale of interest, is due to the late stages in the solvation process and to the equilibrated hydrated electron. (The lifetime of the hydrated electron in air-saturated water is ∼200 ns,[1] with geminate recombination contributions on the picosecond time scale.) Note that these latter species also have weak absorption in the IR, accounting for the long-lived tail of the IR transient signal.

The near-quadratic power dependence of signal amplitude and the consistency of the IR signal decay lifetime when optimally fitted with a variable Gaussian response, over a limited range of pump powers and focusing conditions, lent support to a straightforward interpretation of our transients as reflecting the dynamics of electron solvation. The fitting of a number of these transients yielded a lifetime of the intermediate detected under our experimental conditions of 720 ± 80 fs, with Gaussian response widths ranging from 200 to 400 fs for different experiments. Such response widths appeared reasonable in light of the 115-fs width of the 800-nm fundamental and response broadening dependent on pump−probe overlap geometry in the 5-mm cell. The extracted decay time lies within a wide range of reported lifetimes for the subpicosecond dynamics (from 170 fs to ∼1 ps) measured at a variety of different IR probe wavelengths (not including 1200 nm).[2−11]

Having established the transient behavior in pure water, we proceeded to test the effect of BrdU on the IR signal. BrdU ($C_9H_{11}BrN_2O_5$) from Sigma-Aldrich (99%) was used as supplied, and UV−vis absorption spectra were measured to ascertain the purity and concentration of the BrdU/water solutions before and after transient absorption experiments. Figure 3 is a plot of the measured absorption spectrum of a fresh sample of 0.44 mM BrdU in water in a 5-mm quartz cell, calibrated against our measurement of the BrdU extinction coefficient. (At the 279.5-nm local maximum, $\epsilon = 8790$ M^{-1} cm^{-1}, and at 267 nm, $\epsilon = 6630$ M^{-1} cm^{-1}.) Transients measured with increasing BrdU concentrations but otherwise under fixed experimental conditions (pump energy = 4.46 ± 0.05 μJ/pulse) are shown in Figure 4. The evident progressive shortening of the transient decay, quantified by fitting as before, is clearly suggestive of a dynamic quenching or scavenging of e_{pre}^- in the "bimolecular" scheme mentioned above. (The decrease in absolute amplitude of these signals with increasing BrdU concentration is also expected in the case of scavenging, but attenuation of the pump beam by BrdU absorption at 267 nm must also be considered in this effect; see below.) At the low concentrations at which clear shortening of the transient decay was detected, a sphere of radius larger than 100 Å contains only one BrdU molecule, and scavenging of bulk (randomly distributed) e_{pre}^- would indicate that this species of electron can travel over long distances on the subpicosecond time scale to react with a BrdU molecule.

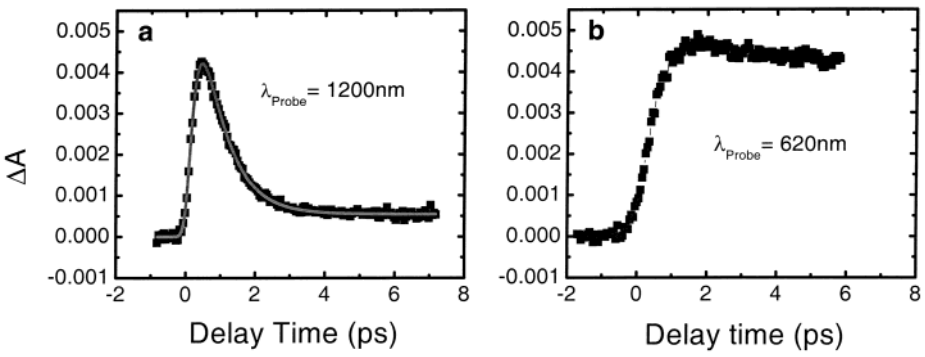

Figure 2. Femtosecond transient absorption measurements, at the probe wavelengths indicated, for 267-nm excitation of pure water in a 5-mm cell.

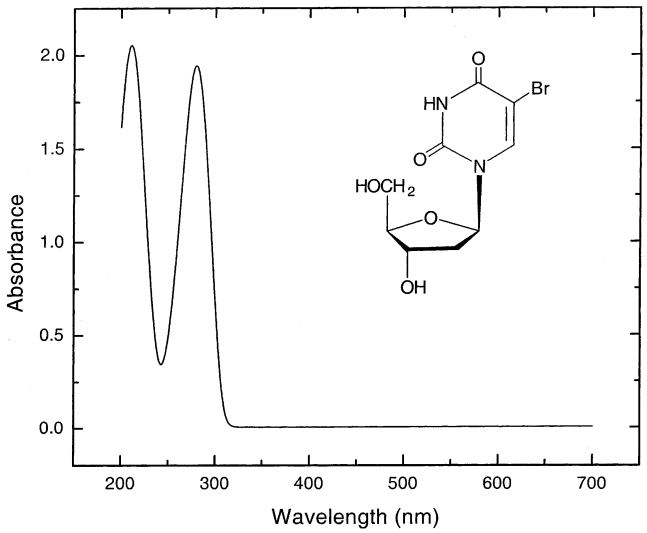

Figure 3. Chemical structure of the electron scavenger 5-bromo-2′-deoxyuridine (BrdU) and its absorption spectrum in water (0.44 mM, 5-mm path length).

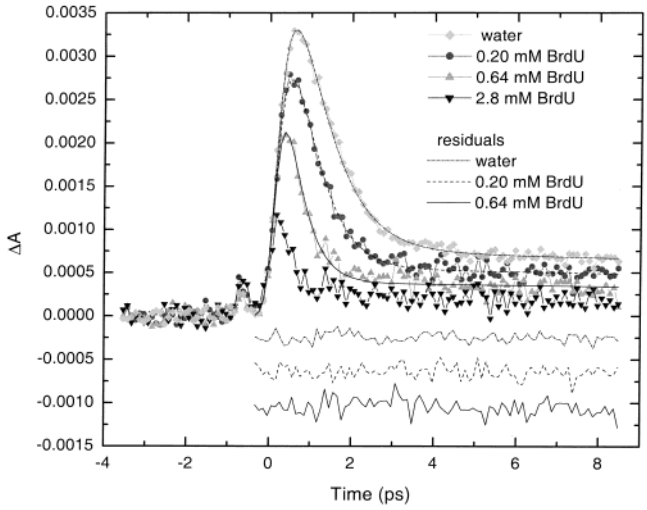

Figure 4. Dependence on BrdU concentration of the femtosecond transient absorption of BrdU/water solutions in a 5-mm cell. Estimated average BrdU concentrations are indicated, on the basis of before and after measurements of static absorption. Also shown are fits of three transients and the residuals of those fits (offset from zero for clarity). See the text for details. The small, concentration-independent peak at negative time is attributed to a coherent response in the front cell window.

Although this possible interpretation is highly intriguing, further analysis of the results revealed several potentially complicating features arising from the strong absorption of the pump pulse energy by BrdU. Foremost among these is a likely concentration dependence of the spatial distribution of the measurement. Because pump−probe timing may vary across a dispersive medium, changes in this distribution introduce the possibility of a systematically changing system temporal response. To determine how significant this effect might be, we have calculated (Figure 5) the effect of BrdU concentration on the spatial distribution of two-photon transitions induced by the pump pulse.

Without BrdU, the pump pulse is attenuated only by small surface reflections and two-photon water absorption across the 5-mm cell. The two-photon absorption rate (number of photons absorbed per second) per water molecule is given by $\delta \cdot \Phi^2$, where Φ is the instantaneous photon flux density (incident photons/cm^2·s) and δ is the two-photon absorption cross section

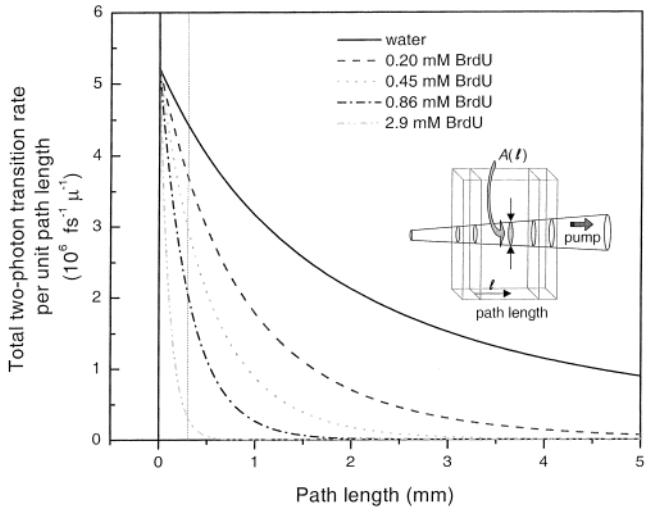

Figure 5. Calculated variation in the two-photon transition rate per unit path length, integrated over the pump beam cross section, *A*, across the 5-mm sample cell for different concentrations of BrdU in water. The illustration shows the pump beam crossing the cell and the dependence of *A* on path length. The following parameters were assumed: 4.46 μJ/pulse, 115-fs pulses, $\delta = 3.79 \times 10^{-51}$ cm^4 s/photon·molecule, $\epsilon = 6630$ M^{-1} cm^{-1}, conical beam with divergence = 2.62° and 13.5 mm from the focus to the sample front surface, and square beam spatial and temporal cross sections. The dotted line is drawn to indicate a depth of 300 μm into the sample.

(cm^4 s/photon·molecule).[28] To calculate the total transition rate (half the rate of photon absorption), $^1/_2\delta \cdot \Phi^2$ is multiplied by the number of molecules in the pump beam; we use an area element *A* that varies across the cell according to beam focusing, as illustrated in Figure 5, and determine the total rate of transitions per unit path length from $^1/_2\delta \cdot \Phi^2 \cdot \rho \cdot A$ where ρ is the number density of water molecules. The highest trace in Figure 5 is the calculated distribution across the pure water sample of the two-photon transition rate estimated for the pump pulse temporal width, energy, and focusing approximating our experimental conditions. The temporal waveform is assumed to be square, and the beam profile is assumed to be uniform to simplify the calculation.

The two-photon absorption cross section of water used in the calculation was determined by reproducing the measured pump beam transmission through the sample. The cross section so-determined at 267 nm (3.8×10^{-51} cm^4 s/photon·molecule) is, given the uncertainties in our approximations, in satisfactory agreement with the cross sections that may be derived from the two-photon absorption coefficients reported elsewhere.[27] Figure 5 shows the instantaneous two-photon transition rate during the assumed square-wave pump pulse, integrated over the pump-beam profile. Thus, for example, in the first 1-μm layer of pure water, after the passage of a 115-fs pulse, 5.2×10^6 fs^{-1} μm^{-1} × 115 fs × 1 μm = 6.0×10^8 two-photon transitions will have occurred. Although attenuation of the pump pulse and the quadratic dependence on light intensity make the number of transitions decay significantly with depth, the distribution extends completely across the cell.

As BrdU is added, the distributions shown in Figure 5 change markedly because of increased attenuation of the pump pulse by BrdU absorption. (The calculated effect of BrdU is based on its one-photon extinction coefficient at 267 nm as given above.) Even at a BrdU concentration of 0.2 mM, the region of significant transition amplitude, and therefore of possible generation of a transient signal, is reduced to the first half of the cell, and for a concentration of 2.9 mM, it is limited to the first few hundred micrometers of the cell.

As mentioned above, the system temporal response is sensitive to the spatial distribution of the measurement because of variations in pump−probe timing across the sample. Although the spatial distribution and amplitude of the actual transient absorption signal depends not only on the pump transition distribution, shown in Figure 5, but also on the alignment and focusing of the probe beam, which selectively maps portions of the pump distribution into the signal distribution, the fact that the pump distribution is not constant means that a constant system temporal response is not assured under the given conditions.

Whereas the changing spatial distribution shown in Figure 5 only raises the possibility of uncertainty due to a changing temporal response function, another feature of the Figure 5 calculations gives a direct indication that the simple dynamic quenching scheme of eqs 1 and 2 is not totally adequate to explain the measurements of Figure 4. The reduction in the absolute number of two-photon water transitions that is predicted to occur in the cell with increasing BrdU concentration should have a clear effect on the amplitude of any transient signal from electrons generated via these transitions. However, an analysis of the data in Figure 4 under the dynamic quenching hypothesis shows that the observed decrease in absolute signal amplitudes as BrdU concentration increases is roughly accounted for by scavenging alone; that is, the inferred initial (time zero) electron yield is at most mildly dependent on BrdU concentration. This is clearly unexpected, unless (1) we are observing signal only from the front surface of the sample (surface effect) where the pump energy is not subject to attenuation or (2) the presence of BrdU enhances the production of electrons as well as scavenging e_{pre}^-. Many solute molecules are known to enhance electron production in this way.

Another complication caused by the strong absorption, coupled with an efficient photolysis channel, is a BrdU concentration that changes during the experiment. Indeed, by measuring changes in absorption spectra and in pump-beam transmission during the course of experiments we could monitor such changes taking place. At concentrations below 1 mM in a volume of 0.5 mL, the change in concentration is significant even for experiments in which the sample is irradiated for only a matter of minutes. Although the cells where subjected to constant stirring, it was also clear from pump-beam transmission measurements that persistent local inhomogeneities in the concentrations of BrdU and its photoproducts were quickly generated by the irradiation. A precise determination of the effective local BrdU concentration producing any observed effect was therefore not possible on the basis of absorption spectra measurements. In addition, strong absorption gives rise to a nonnegligible BrdU excited state and photoproduct concentration, and a role for these species in any observed effect could not be excluded.

The above-delineated ambiguities and uncertainties associated with the cell experiments can be largely eliminated by performing the experiments in a sample jet of 300-μm thickness. In this arrangement, homogeneity is assured as the sample is replaced for each laser shot, and the effect of photolysis on BrdU concentration is reduced 1000-fold by the use of a 0.5-L sample reservoir. Although the variation in spatial distribution is not completely eliminated for the range of BrdU concentrations of interest (see, e.g., the first 300-μm sample layer in Figure 5), the possible magnitude of any dispersive effect on the temporal response is greatly reduced by limiting the maximum pump−probe overlap path length to 300 μm. Finally, the jet is free of the possibility of surface effects from molecules adhering to the quartz−water interface.

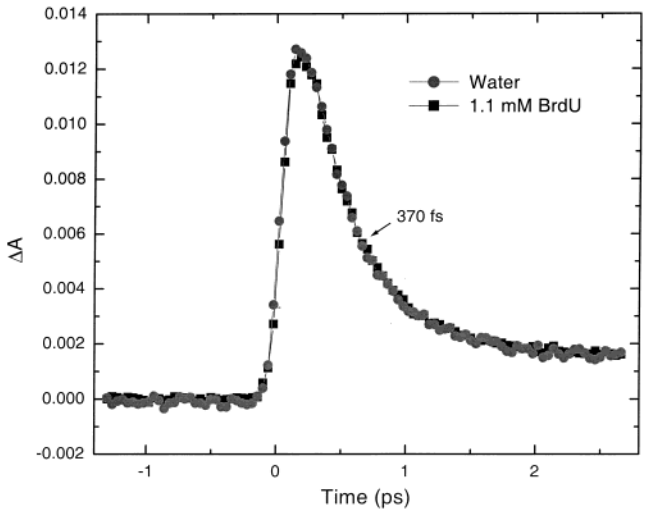

Figure 6. Femtosecond transient absorption measurements in a 300-μm jet of pure water and 1.1 mM BrdU in water. The lifetime of the principle decay component is shown.

Measurements carried out in the jet under fixed experimental conditions on a pure water sample and 1.1 mM BrdU in water are shown in Figure 6. The pump power was 0.46 μJ/pulse with an estimated pulse length and beam diameter of 85 fs and 140 μm for a maximum photon flux density 2 to 3 times higher than that in the cell experiment. The concentration and purity of the BrdU solution in the sample reservoir were monitored by absorption spectra. The pump and probe wavelengths were again 267 and 1200 nm. The pure water transient is dramatically different from that recorded in the cell, and no effect of BrdU on the dynamics is resolvable. The measured signal amplitude in BrdU is 4% lower, a change within the level of experimental variation expected from limitations on the degree of precision with which a constant pump power could be maintained. The common parameters determined from these data sets indicate a 90 ± 10 fs rise time and a 370 ± 30 fs fast decay (for a 120-fs fwhm Gaussian response). These values are similar to those determined from the first experiment showing evidence of e_{pre}^-, which was performed with a pump wavelength of 310 nm and a probe wavelength of 1250 nm.[2] An appearance time of 110 fs and a decay lifetime of 240 fs were reported from that work.

These results show conclusively that the suspected long-range scavenging of e_{pre}^- by BrdU does not occur. In fact, no detectable effect was observed in further experiments with BrdU concentrations of up to 10 mM. In addition, the near constancy of the transient signal amplitude for pure water and for 1.1 mM BrdU, despite the BrdU absorption of pump light (BrdU reduced the measured pump pulse transmission through the jet by one-third), can now be cleanly ascribed to the enhancement of electron production by the BrdU molecules. Given the two-photon nature of the electron production and the fact that the pump−probe overlap region was shown to be several hundred micrometers in length by translating the sample at fixed alignment, a 32% drop in signal would be predicted if the only effect of BrdU were to attenuate the pump beam. Even if only the first 100 μm of the sample were probed, BrdU absorption would reduce the signal by 15%.

Finally, the origin of the striking concentration dependence in the cell remains to be explained. As we will show below, we believe that this dependence is the result of changes in the temporal response caused by the variation in spatial distribution

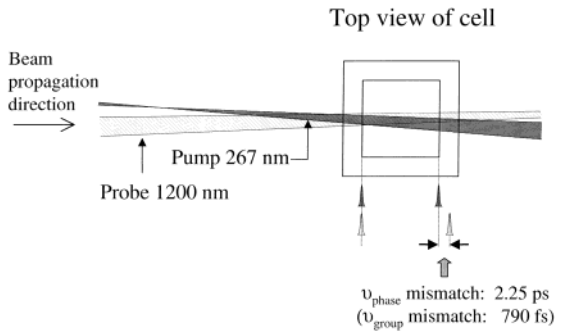

Figure 7. Approximate alignment and focusing of pump and probe beams crossing the 5-mm sample cell in the cell experiments. The transit time mismatch of pump and probe pulses is shown schematically for pulses entering the sample at the same time.

illustrated in Figure 5, coupled with the velocity difference between pump and probe pulses as they transit the cell. As an initial indication of the dispersion effect, the indices of refraction of water at 267 and 1200 nm were evaluated on the basis of the formulation of Schiebener et al.:[29] $n_{267\ nm} = 1.3693$ and $n_{1200\ nm} = 1.3219$ at $T = 25$ °C. These numbers indicate a *phase* velocity transit time mismatch across a 5-mm cell of $\Delta t = (\Delta n \cdot 5\ \text{mm})/c = 790$ fs, with the pump slower than the probe. If this value reflected the pulse transit times, then the time zero for the signal from the front surface layer of sample would be 790 fs earlier than the time zero for the final layer at the back window of the cell. The signals from successive layers across the cell, which, for equal probing, would decay in amplitude as a function of depth as seen in Figure 5, would thus be spread in time, giving an artificial smearing out of the transient signal. This smearing changes with BrdU concentration and can be represented by a response function derived by converting the Figure 5 spatial distributions to temporal distributions based on the transit time differential. Simulations in which this was done for a 5-mm transit time spread of 790 fs, under the assumption of constant electron transient behavior of the form determined from the jet measurements, do not produce anything approaching the pronounced concentration dependence observed in the cell.

In fact, however, the propagation of a pulse envelope in a dispersive medium is governed by the *group* velocity because of the systematic variation in phase velocity with frequency across the frequency spectrum of the pulse.[30,31] Thus, the actual pulse transit time mismatch is $\Delta t_g = (\Delta n_g \cdot 5\ \text{mm})/c$, where the group velocity index is defined as[31] $n_g = c/v_g$, from which the relation $n_g = n - \lambda_{vac} \cdot dn/d\lambda_{vac}$ can be derived, where λ_{vac} is the vacuum wavelength. The distinction between group and phase velocity does not give rise to a significant change in calculated Δt for wavelengths across the visible and near-IR, for which $dn/d\lambda_{vac}$ is small and $\lambda_{vac} \cdot dn/d\lambda_{vac}$ changes slowly. For example, $\lambda_{vac} \cdot dn/d\lambda_{vac} = -0.0178$ at 600 nm and -0.0197 at 1200 nm, meaning that Δn_g differs from Δn by only 0.0019, corresponding to a change in Δt for a 5-mm path of only 32 fs.

However, the effect is quite dramatic in the present case because of the UV pump wavelength and the large magnitude of $dn/d\lambda_{vac}$ in the UV; at 267 nm, $\lambda_{vac} \cdot dn/d\lambda_{vac} = -0.1075$, making Δn_g for 267 nm/1200 nm 3 times as large as the corresponding Δn. That is, $n_{g\ 267\ nm} = 1.4768$, $n_{g\ 1200\ nm} = 1.3416$, $\Delta n_g = 0.135$, and $\Delta t_g = 2.25$ ps over 5 mm. An experimental determination of the n_g value of water for our pump pulse yielded 1.479(3), confirming the calculated result.

With a Δt_g of this order and a pump/probe overlap volume stretching across most of the cell, consistent with our experimental geometry (see Figure 7), simulations can give a very satisfactory approximation of our cell observations. The length of the overlap is determined by the beam diameters and the crossing angle of the beams, here dictated by the use of a single focusing lens for both pump and probe. Simulations of the type described above, in which electron dynamics are constant but changing BrdU concentration causes a changing signal spatial distribution, are shown in Figure 8 for $\Delta t_g(5\ \text{mm}) = 2.5$ ps. An intrinsic pulse cross-correlation of 190 fs was included in the response function, and the probe alignment walk-off from optimum alignment at the front surface of the sample was approximated by an additional decay in the signal intensity across the cell (exponential with a length constant of 2.5 mm).

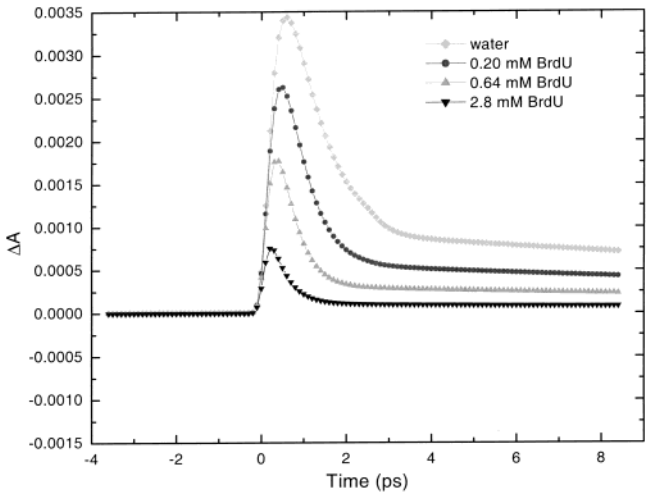

Figure 8. Simulation of the concentration dependence of the femtosecond transient absorption of BrdU/water solutions in a 5-mm cell. It is assumed that the only effect of BrdU is the attenuation of the pump beam. See the text for details.

Although a quantitative reproduction of the experimental data is not intended, given the many approximations involved, the simulation demonstrates clearly that the group velocity effect can account for the major concentration dependence observed in the cell. It should be noted that group velocity, equal to $1/(dk/d\omega)$ where $k = 2\pi/\lambda$, would be independent of wavelength if $d^2k/d\omega^2$ were zero. A nonzero value for this second derivative allows the group velocity of our pump and probe pulses to differ, and the same $d^2k/d\omega^2$, often referred to simply as the "group velocity dispersion," also governs pulse broadening in ultrashort pulse experiments.[32] (For 85-fs pulses in water, the broadening over 5 mm is minor. At 267 nm, $d^2k/d\omega^2 = 206$ fs^2/mm, and an 85-fs transform-limited Gaussian pulse broadens to 91.4 fs.)

It is interesting to observe that the time scale of the decay of the highest concentration transients in Figures 4 and 8 agree well with the intrinsic e_{pre}^- dynamics measured in the jet (Figure 6). This can be attributed to the fact, illustrated in Figure 5, that the signal at such concentrations is generated almost entirely within a 300-μm sheet of water at the front surface of the cell; therefore, the group-velocity mismatch has a minimal effect, just as in the jet.

One difference that is readily noted between the simulations of Figure 8 and the experiment of Figure 4 is that the experimental amplitudes exceed those of the simulations (for which a single normalization factor was chosen to match simulation to experiment for pure water) by progressively larger factors as the concentration increases. This is consistent with the conclusion drawn from the jet measurements that BrdU does not simply serve to attenuate the pump power, which is the only role accorded it in the simulation, but also enhances electron

production. It is then natural to find that the degree of enhancement grows more or less linearly with concentration.

As further confirmation of the electron-generation enhancement effect of BrdU, an absolute increase in the solvated electron (e_{solv}^-) signal, measured 5 to 10 ps after the pump pulse, was seen with increasing BrdU concentration in experiments with a pump wavelength of 310 nm and probe wavelength of 1000 nm. These experiments were also performed in a 5-mm cell, with pump pulse attenuation by BrdU absorption greatly reduced by an extinction coefficient at 310 nm that is 16 times lower than at 267 nm. For 4 mM BrdU in water, the measured solvated electron signal (at pump−probe delays greater than 4 ps) was about double that from pure water. The actual enhancement must be larger than this because pump attenuation is still a significant factor at this concentration, even at 310 nm. In light of this result, the nearly identical amplitudes of the transients measured in the jet for water and for 1.1 mM BrdU in water appear to reflect only a coincidental balance between the reduction from pump attenuation and the BrdU enhancement effect. The absence in the jet of any change in transient shape may be more significant, suggesting that those electrons produced via the more efficient channel associated with the presence of BrdU exhibit very similar dynamic behavior to that of electrons generated from pure bulk water.

In conclusion, we have found that e_{pre}^- is not scavenged by BrdU at the studied concentrations but that BrdU does enhance electron production for 267- and 310-nm irradiation of water. The plausible indications of a scavenging effect observed in measurements in a 5-mm cell emphasize the potential for a combination of experimental factors—near-collinear pump−probe alignment, large beam diameters, UV excitation, and strong BrdU absorption—to produce misleading results. The present case illustrates in particular the need for added caution in interpreting time-resolved experiments in condensed media when a direct, in-situ measurement of the instrument temporal response is difficult to obtain and spatial distribution and group-velocity differences are involved.

Acknowledgment. This work was supported by the National Science Foundation.

References and Notes

(1) Hart, E. J.; Anbar, M. *The Hydrated Electron*; Wiley-Interscience: New York, 1970.

(2) Migus, A.; Gauduel, Y.; Martin, J. L.; Antonetti, A. *Phys. Rev. Lett.* **1987**, *58*, 1559.

(3) Long, F. H.; Lu, H.; Eisenthal, K. B. *Phys. Rev. Lett.* **1990**, *64*, 1469.

(4) Silva, C.; Walhout, P. K.; Yokoyama, K.; Barbara, P. F. *Phys. Rev. Lett.* **1998**, *80*, 1086.

(5) Baltuška, A.; Emde, M. F.; Pshenichnikov, M. S.; Wiersma, D. A. *J. Phys. Chem. A* **1999**, *103*, 10065.

(6) Hertwig, A.; Hippler, H.; Unterreiner, A.-N. *Phys. Chem. Chem. Phys.* **2002**, *4*, 4412.

(7) Kambhampati, P.; Son, D. H.; Kee, T. W.; Barbara, P. F. *J. Phys. Chem. A* **2002**, *106*, 2374.

(8) Assel, M.; Laenen, R.; Laubereau, A. *Chem. Phys. Lett.* **2000**, *317*, 13.

(9) Laenen, R.; Roth, T.; Laubereau, A. *Phys. Rev. Lett.* **2000**, *85*, 50.

(10) Laenen, R.; Roth, T. *J. Mol. Struct.* **2001**, *598*, 37.

(11) Anderson, N. A.; Hang, K.; Asbury, J. B.; Lian, T. *Chem. Phys. Lett.* **2000**, *329*, 386.

(12) Yang, C.-Y.; Wong, K. F.; Skaf, M. S.; Rossky, P. J. *J. Chem. Phys.* **2001**, *114*, 3598, and references therein.

(13) Borgis D.; Bratos, S. *J. Chem. Phys.* **1997**, *437*, 537, and references therein.

(14) Goulet, T.; Bernas, A.; Ferradini, C.; Jay-Gerin J.-P. *Chem. Phys. Lett.* **1990**, *170*, 492.

(15) Bernas, A.; Ferradini, C.; Jay-Gerin, J.-P. *Chem. Phys.* **1997**, *222*, 151.

(16) Bartels, D. M.; Crowell, R. A. *J. Phys. Chem. A* **2000**, *104*, 3349.

(17) Lu, Q.-B.; Sanche, L. *Phys. Rev. B* **2001**, *63*, 153403.

(18) Lu, Q.-B.; Sanche, L. *Phys. Rev. Lett.* **2001**, *87*, 078501.

(19) Jonah, C. D.; Miller, J. R.; Matheson, M. S. *J. Phys. Chem.* **1997**, *81*, 11618.

(20) Pimblott, S. M.; LaVerne, J. A. *J. Phys. Chem. A* **1998**, *102*, 2967.

(21) Kee, T. W.; Son, D. H.; Kambhampati, P.; Barbara, P. F. *J. Phys. Chem. A* **2001**, *105*, 8434.

(22) Wan, C.; Fiebig, T.; Kelley, S. O.; Treadway, C. R.; Barton, J. K.; Zewail, A. H. *Proc. Natl. Acad. Sci. U.S.A.* **1999**, *96*, 6014.

(23) Fiebig, T.; Wan, C.; Zewail, A. H. *ChemPhysChem* **2002**, *3*, 781.

(24) Hutchinson, F. *Q. Rev. Biophys.* **1973**, *6*, 201.

(25) Shetlar, M. D. *Photochem. Photobiol. Rev.* **1980**, *5*, 105.

(26) Rivera, E.; Schuler, R. H. *J. Phys. Chem.* **1987**, *87*, 3966.

(27) Nikogosyan, D. N.; Oraevsky, A. A.; Rupasov, V. I. *Chem. Phys.* **1983**, *77*, 131−143. Dragonmir, A.; McInerney, J. G.; Nikogosyan, D. N. *Appl. Opt.* **2002**, *41*, 4365−4376.

(28) McClain, W. M. *Acc. Chem. Res.* **1974**, *7*, 129.

(29) Schiebener, P.; Straub, J.; Levelt Sengers, J. M. H.; Gallagher, J. S. *J. Phys. Chem. Ref. Data* **1990**, *19*, 677 and 1617.

(30) Siegman, A. E. *Lasers*; University Science Books: Mill Valley, CA, 1986; p 337.

(31) Hecht, E.; Zajac, A. *Optics*; Addison-Wesley: Reading, MA, 1974; pp 204, 205.

(32) Siegman, A. E. *Lasers*; University Science Books: Mill Valley, CA, 1986; p 356.